Journal of Alloys and Compounds 514 (2012) 25–29

Contents lists available at SciVerse ScienceDirect

Journal of Alloys and Compounds

journal homepage: www.elsevier.com/locate/jallcom

Exchange bias effect of $Co_{3-x}Fe_xO_4$ ($x = 0$, 0.09, 0.14 and 0.27)

Yue Zhang[a], Zhi Yang[b], Ben-Peng Zhu[a], Jun Ou-Yang[a], Rui Xiong[b], Xiao-Fei Yang[a], Shi Chen[a,*]

[a] Department of Electric Science and Technology, Huazhong University of Science and Technology, Wuhan 430074, China
[b] Key Laboratory of Artificial Micro- and Nano-structures of Ministry of Education and School of Physics and Technology, Wuhan University, Wuhan 430072, China

ARTICLE INFO

Article history:
Received 24 August 2011
Received in revised form
22 September 2011
Accepted 28 September 2011
Available online 4 October 2011

Keywords:
Exchange bias effect
Fe doped Co_3O_4
Magnetic measurements

ABSTRACT

$Co_{3-x}Fe_xO_4$ ($x = 0$, 0.09, 0.14 and 0.27) powders were synthesized by the thermal-decomposition method with annealing treatment. With the increase of x, the composition of the products experiences a transition from the single-phase compound of $Co_{3-x}Fe_xO_4$ to the coexisted phases of $Co_{3-x}Fe_xO_4$ and $CoFe_2O_4$, which is accompanied with the enhancement of the ferromagnetic (FM) response. In addition, the horizontal negative exchange bias (EB) effect was observed in the Fe^{3+} doped samples. For $Co_{3-x}Fe_xO_4$ with $x = 0.09$ and 0.14, the EB fields at 10 K are larger than 100 Oe, and the EB effect disappears as temperature is above 30 K, close to the Néel temperature for the antiferromagnetic (AFM) Co_3O_4. While for $Co_{3-x}Fe_xO_4$ with $x = 0.27$, the EB field at 10 K weakens clearly, but the EB effect finally disappears as temperature increases to 200 K. These results indicate that the EB effect for $Co_{3-x}Fe_xO_4$ with $x = 0.09$ and 0.14 are mainly related with the exchange coupling at the FM/AFM interfaces, while for $x = 0.27$, the decoupling of the FM and AFM phases may occur.

1. Introduction

The exchange bias (EB) effect, which was firstly observed in 1956 [1], refers to the shift of a hysteresis loop, which is related with the competitive exchange interaction at the interfaces of different kinds of nano-sized magnetic materials, such as the exchange bonding at the interfaces between the ferro-/ferrimagnetic (FM) and the antiferromagnetic (AFM) nano-materials, or between the FM cores and the frozen surface spin-glasslike (SGL) states in some FM nano-particles. As these samples are cooled under a field from a temperature higher than the Néel temperature (T_N) of the AFM phase (or the freezing temperature (T_f) of SGL state) to a lower temperature, the spins at the FM/AFM or FM/SGL interfaces will be pinned in the direction of the external field (the so-called unidirectional anisotropy), and an external energy is necessary for reversing these pinned spins, which leads to the horizontal shift of the loop.

In recent years, the EB effect has attracted studying interest due to its potential application in the field of information storage [2,3]. Up to now, the EB effect has been observed in a lot of materials with composite magnetic structures, including (1) the FM/AFM composite films, such as $Ni_{81}Fe_{19}$/CoO [4], Fe/FeF_2 [5,6], Fe/MnF_2 [6], (Fe, Co, Ni)/CoO [7], Co/Co_3O_4 [8], $Ni_{80}Fe_{20}$/Co_3O_4 [9], Ni/Co_3O_4 [10], (2) the FM nano-particles embedded in the AFM matrices or FM(core)/AFM(shell) composite nano-particles, such as Co/CoO [1,3,11], Fe/Fe_2O_3 [12–14], Ni/NiO [15], $CoFe_2O_4$/NiO [16], $CuFe_2O_4$/NiO [17], $CoFe_2O_4$/CoO [18], and a review by Nogués et al. [19] gives a detail discussion on the EB effect in this kind of FM/AFM composite materials, and (3) the FM nano-particles with SGL spins near the surfaces, such as $CoFe_2O_4$ [20–22], $NiFe_2O_4$ [23–25], γ-Fe_2O_3 [26].

Among these composite materials, the FM and AFM(SGL) phases are separated, and the FM/AFM(SGL) interfaces are mainly formed by some special methods, such as mechanic balling [24,25], oxygen passivation [1,12–15] and some chemical methods [16–18]. While it is also predictable that the FM/AFM(SGL) interfaces may also be induced by doping magnetic ions in the AFM compound, since this can break the AFM exchange coupling, cause the canting of the moments near the doping sites, and induce the net FM moments and the competition between the FM and AFM interactions. For example, it is reported that by doping Fe ions in the AFM compound NiO, an EB effect is observed [27].

In the present work, the EB effect in the Fe doped Co_3O_4 has been studied in detail. Co_3O_4 was chosen due to its easy fabrication, as well as the related works concerning the EB effect in Co_3O_4 and the related composite materials [8–10,28,29].

2. Experimental methods

The raw materials for synthesizing cobalt ferrite nano-particles are $Co(NO_3)_2{\cdot}6H_2O$, $Fe(NO_3)_3{\cdot}9H_2O$ and oleylamine. All of the reagents used in the experiments are of analytical grade and used without further purification.

* Corresponding author at: Luoyu Road 1037#, Wuhan, Hubei, China. Tel.: +86 27 87542893; fax: +86 27 87558209.
E-mail address: s_chen@mail.hust.edu.cn (S. Chen).

0925-8388/$ – see front matter © 2011 Published by Elsevier B.V.
doi:10.1016/j.jallcom.2011.09.077

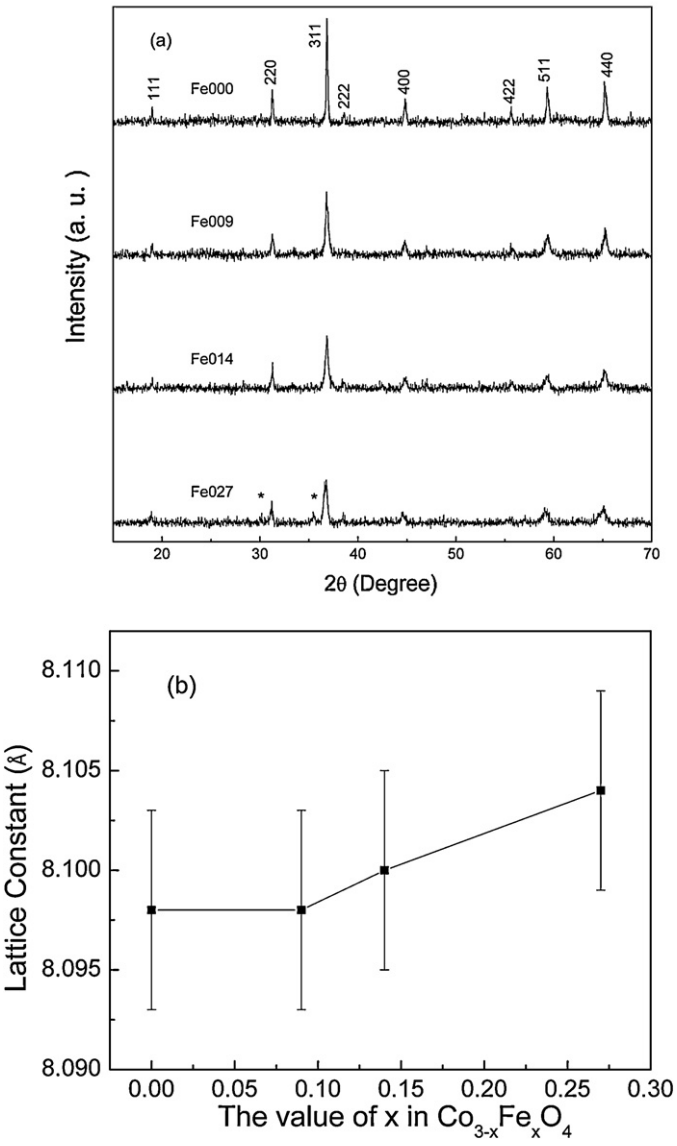

Fig. 1. (a) The XRD patterns for $Co_{3-x}Fe_xO_4$ (x = 0, 0.09, 0.14 and 0.27) powders. (b) The change of the lattice constants with the doping content of the Fe^{3+} ions in $Co_{3-x}Fe_xO_4$ (x = 0, 0.09, 0.14 and 0.27) powders.

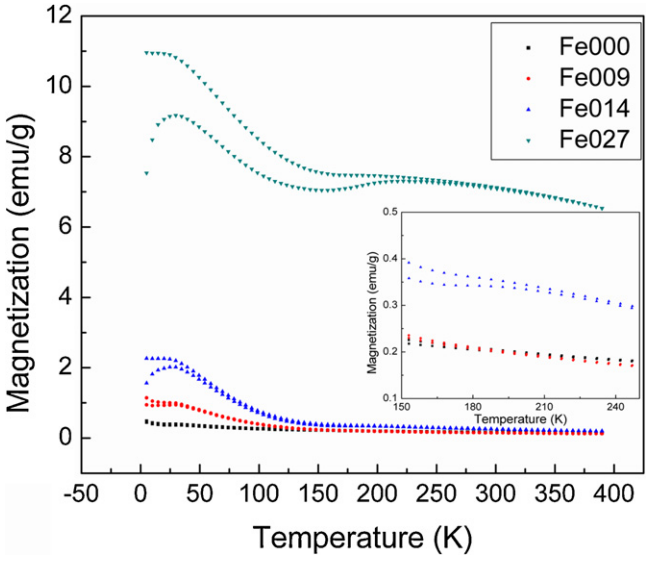

Fig. 2. The ZFC–FC magnetization for $Co_{3-x}Fe_xO_4$ (x = 0, 0.09, 0.14 and 0.27) powders, the inset shows the close-up view of the curves for $Co_{3-x}Fe_xO_4$ (x = 0, 0.09 and 0.14) between 150 and 250 K.

Firstly, the precursor powders were synthesized by the thermal-decomposition method according to Ref. [30]. Then the final products of $Co_{3-x}Fe_xO_4$ (x = 0, 0.09, 0.14 and 0.27) were obtained by annealing the precursor powders at 873 K for 5 h. The samples were named by Fe000, Fe009, Fe014 and Fe027 according to the amount of the doped Fe^{3+} ions.

X-ray diffraction (XRD, D8-Advanced) phase analysis was performed by using Cu Kα radiation in a 2θ scanning from 15° to 70° (1°/min) at a step of 0.02°. The magnetic measurements were carried out by using a vibrating sample magnetometer (VSM) on a physical property measure system (PPMS-9 Quantum Design). The magnetization–temperature (M–T) curves were measured with the zero-field-cooling (ZFC) and FC procedures under the field of 5000 Oe. The hysteresis loops were collected at 300 K, 250 K, 200 K, 150 K, 100 K, 50 K, 30 K, 20 K and 10 K with the FC procedure from 350 K to these temperatures under the field of 5000 Oe. For comparison, the ZFC loops were also collected at 10 K.

3. Results and discussion

The XRD spectra of the pure and Fe-doped samples are shown in Fig. 1(a). It can be seen that the peak positions of sample Fe000 are close to the data in the Committee for Powder Diffraction Standard (JCPDS) for Co_3O_4 (No. 43-1003). This indicates the formation of the single-phase Co_3O_4. In the XRD patterns for samples Fe009, Fe014 and Fe027, the peak intensity weakens, which is ascribed to the destroyed lattice near the doping sites. In addition, for sample Fe027, the second phase of $CoFe_2O_4$ (JCPDS card: 22-1086) is also detected (labeled as *).

By the positions of the strongest (3 1 1) peaks, the lattice constants were determined by using the well known Bragg equation, and the results are shown in Fig. 1(b). It can be seen that the lattice constants show a small increase with the increasing content of the doped Fe^{3+} ions, whose radius, 0.645 Å, is a little larger than that of Co^{3+} ion (0.60 Å) [31].

In the M–T curves shown in Fig. 2, with the increase of the doping content, the great enhancement of magnetization is seen. In addition, it is also noticed that for sample Fe000, the ZFC and FC curves are almost overlapped, while for the samples with the doped Fe ions, the bifurcation of the ZFC and FC branches occurs below certain temperatures (named as T_B), and the T_B shifts to the higher temperatures with the increase of the doping content. These results indicate that the doping of Fe^{3+} ions induces the short-range FM orders and the formation of the FM $CoFe_2O_4$ nano-particles in sample Fe027 enhances the FM response greatly. Furthermore, in the M–T curves of samples Fe000 and Fe009, peaks appear at about 30 K, and for samples Fe014 and Fe027, such peaks shift to about 25 K. In addition, in the ZFC curve for sample Fe027, another broad peak is clearly detected near 220 K, and as shown in the inset figure, in sample Fe014, a very weak peak is also detected near 200 K. The peaks near 30 K are close to the T_N of Co_3O_4 [28,29], which indicates the transition between AFM and paramagnetic state, and the small shift of T_N for samples Fe014 and Fe027 may be ascribed to the destroyed AFM couplings due to the increase of the doping content. For sample Fe027, the broad peak near 220 K may be related with the transition between the blocked FM state and the superparamagnetic state for the formed $CoFe_2O_4$ nano-particles [32], which are detected by XRD, while in sample Fe014, the size or content of such second phase may be so small that they cannot been detected by XRD, but only a weak peak is detected in the ZFC curve.

The ZFC and FC magnetic hysteresis loops measured at 10 K for samples Fe000, Fe009, Fe014 and Fe027 are shown in Fig. 3(a)–(d), respectively. It can be seen that for samples Fe000, Fe009, and Fe014, the magnetization near 30,000 Oe is reversible, which

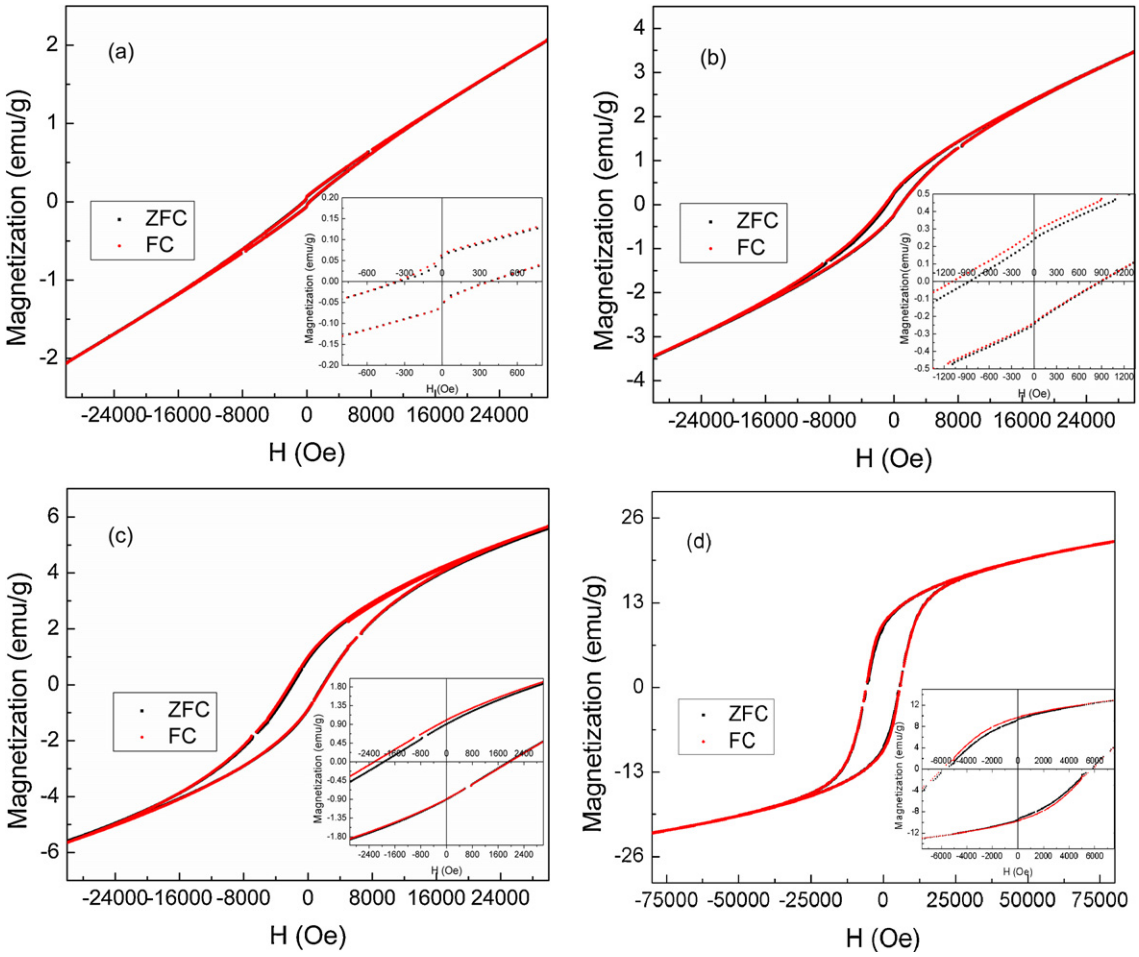

Fig. 3. The magnetic hysteresis loops measured at 10 K by ZFC and FC procedures for $Co_{3-x}Fe_xO_4$ powders with (a) $x = 0$, (b) $x = 0.009$, (c) $x = 0.14$ and (d) $x = 0.27$. The inset figures show the close-up view of the loops near $M = 0$ emu/g for a clear observation on the loop shift.

indicates that for these three samples, this 30,000-Oe field is sufficient to surpass the irreversibility field in the FM phase, while for sample Fe027, the loop near 30,000 Oe is open, which is due to the larger anisotropy energy at the lower temperature for $CoFe_2O_4$ with larger size. In this case, the loop can also shift after the FC process, which is the so-called minor loop effect [33,34], but not the EB effect. Therefore, for sample Fe027, the maximum applied field is increased to 80,000 Oe, which, as shown in Fig. 3(d), seems to be large enough to surpass the anisotropy field of $CoFe_2O_4$.

From the loops in Fig. 3, the coercivity (H_C) and the EB field (H_e) are determined by fitting the data near $M = 0$ emu/g. Let H_{C1} and H_{C2} be the fitted intercepts at the negative and positive axis, respectively, $H_C = (H_{C2} - H_{C1})/2$ and $H_e = (H_{C2} + H_{C1})/2$. Therefore, if H_e is smaller than zero, the loops have negative shift, and vice versa. The values of H_C and H_e are all listed in Table 1.

Table 1
The magnetic properties measured at 10 K for $Co_{3-x}Fe_xO_4$ ($x = 0$, 0.09, 0.14 and 0.27) powders.

Sample	H_C (ZFC)/Oe	H_C (FC)/Oe	H_e/Oe
Fe000	359 ± 2	378 ± 3	10 ± 2
Fe009	880 ± 2	984 ± 3	−104 ± 2
Fe014	1932 ± 2	2096 ± 2	−139 ± 1
Fe027	5695 ± 6	5856 ± 9	−70 ± 9

As can be seen in Fig. 3, the hysteresis loops of sample Fe000 show clear AFM characterization, such as the linear shape, the small magnetization under the field as large as 30,000 Oe and the small coercivity. While the doping of Fe ions induces the bending of the loops, as well as the great enhancement of coercivity and magnetization, which indicates the appearance and enhancement of the FM response. In addition, for sample Fe000, the ZFC and FC loops are almost overlapped, while for samples Fe009 and Fe014, in comparison with the ZFC loops, the FC loops show clear horizontal negative shifts, for sample Fe027, the loop shift becomes clearly smaller. From Table 1, it is shown that the values of H_e for samples Fe009 and Fe014 are larger than 100 Oe, and the H_e of sample Fe014 is larger, about 139 Oe, while the H_e for sample Fe027 is only 70 Oe, and for these samples, the values of H_C with FC procedures are about 100–200 Oe larger than those with ZFC procedures. These results indicate the EB effect for the Fe doped samples, and the changes of H_e may reflect the changed areas of the FM/AFM interfaces, which is decided by the amount and size of the FM phase. For sample Fe009, due to the small doping content, the amount and size of the FM phase is small, which may lead to the smaller areas of the FM/AFM interfaces, and the EB effect is not very strong, for sample Fe014, the areas of the FM/AFM interfaces may increase due to the increased amount of the FM phase with still small size, and thus the EB effect is relatively stronger. For sample Fe027, since the doped Fe ions induce the formation of the second phase of $CoFe_2O_4$ nano-particles with the larger amount and sizes, which may decrease the areas of the FM/AFM interfaces greatly, and thus weakens the EB effect.

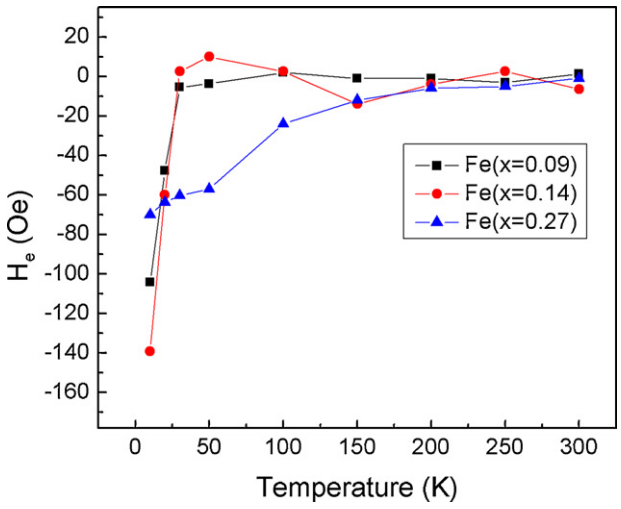

Fig. 4. The temperature dependence of H_e for $Co_{3-x}Fe_xO_4$ (x = 0.09, 0.14, and 0.27) powders.

In sample Fe027, it is clear that the enhanced FM response is contributed from the $CoFe_2O_4$ nano-particles. In samples Fe009 and Fe014, even though the FM phase cannot be detected by XRD, from the characteristic M–T curves for samples Fe014 and Fe027, it is reasonable that the FM response should also be related with $CoFe_2O_4$, and its amount can be roughly estimated by the M–H curves: Since the susceptibility of the AFM Co_3O_4 is several magnitudes smaller than that of $CoFe_2O_4$, the magnetization contributed from Co_3O_4 is negligible, and it seems that near 30,000 Oe, the M–H curves have become straight lines, which indicates the magnetization saturation for $CoFe_2O_4$. Therefore, by the known sample masses and the saturation magnetization for $CoFe_2O_4$ (about 80 emu/g [35]), the amount of the $CoFe_2O_4$ was estimated by removing the high-field susceptibility, the results show that in sample Fe009, the amount of $CoFe_2O_4$ is about 1.2%, and in sample Fe014, it is about 3.1%, both are indeed not larger than the detection limit for XRD.

The temperature dependence of H_e is shown in Fig. 4. It is clear that for samples Fe009 and Fe014, the values of H_e decrease greatly with temperature increasing from 10 K to 30 K, and as temperature is higher than 30 K, it seems that little shift is observed. Since the T_N of Co_3O_4 is close to 30 K, it can be concluded that in samples Fe009 and Fe014, the EB effect is related with the exchange coupling at the FM/AFM interfaces. For sample Fe027, even though the H_e at 10 K is obviously smaller, the values of H_e decrease smoothly with the increase of temperature. As temperature is higher than 30 K, the shifts can still be observed, and finally disappear above 200 K, which is near the blocking temperature shown in the ZFC M–T curve. This indicates that in sample Fe027, the coupling between the FM and AFM phases may be destroyed due to the formation and crystallization of the FM $CoFe_2O_4$ nano-particles with larger sizes. While the mechanism for this small loop-shift phenomenon is complicated: for the FM nano-particles, the frozen surface SGL state can also cause the EB effect, but it is generally reported that in ferrite nano-particles such EB effect appear at the very low temperature (usually lower than 50 K), and will disappear as temperature is higher than the freezing temperature for the SGL state [20–26], but in the present work, for sample Fe027, the loop shift reduces slowly with temperature increasing and finally disappears above 200 K, i.e. the small loop shift can be observed if only the $CoFe_2O_4$ nano-particles are in a blocked FM state. Therefore, we think that this small loop shift in sample Fe027 may not be the general EB effect, but may be ascribed to some other mechanisms. Since in sample Fe027, even though the strong exchange bonding between $CoFe_2O_4$ and Co_3O_4 is destroyed, both phases still co-exist in the final products, and the weaker inter-particle interaction, such as the dipole interaction, may still exist, which can cause the so-called "magnetic proximity effect" [36] or "magnetic stability effect" [37], and can also induce a small loop shift. This weak EB-like effect in the composite magnetic materials without strong interface exchange bond deserves the further research.

4. Conclusions

The content of the doped Fe^{3+} ions in $Co_{3-x}Fe_xO_4$ (x = 0, 0.09, 0.14 and 0.27) has great impact on the composition and magnetic properties. The enhancement of the FM response with the increasing content of the Fe^{3+} ions is observed due to the formation of the FM phase. In addition, for samples Fe009 and Fe014, the horizontal negative shifts occur due to the exchange interactions at the FM/AFM interfaces, while in sample Fe027, the $CoFe_2O_4$ second phases are observed, and the FM/AFM coupling is destroyed.

Acknowledgments

The authors would like to acknowledge the financial support from Chinese National Foundation of Natural Science (No. 10974148, 60871018, 61106005 and 51172166), 973 Program (2009CB939705) and NSFC (Grant 51002055).

References

[1] W.H. Meiklejohn, C.P. Bean, Phys. Rev. 102 (1956) 1413–1414.
[2] B. Dieny, V.S. Speriosu, S.S.P. Parkin, B.A. Gurney, D.R. Wilhoit, D. Mauri, Phys. Rev. B 43 (1991) 1297–1300.
[3] V. Skumryev, S. Stoyanov, Y. Zhang, G. Hadjipanayis, D. Givord, J. Nogués, Nature 423 (2003) 850–853.
[4] K. Takano, R.H. Kodama, A.E. Berkowitz, Phys. Rev. Lett. 79 (1997) 1130–1133.
[5] J. Nogués, D. Lederman, T.J. Moran, I.K. Schuller, Phys. Rev. Lett. 76 (1996) 4624–4627.
[6] J. Nogués, C. Leighton, I.K. Schuller, Phys. Rev. B 61 (2000) 1315–1317.
[7] M. Gruyters, Phys. Rev. B 79 (2009) 134415.
[8] B. You, Y.X. Wang, Y.L. Zhao, L. Sun, W.T. Sheng, M.H. Pan, J. Du, J. Appl. Phys. 93 (2003) 6587–6589.
[9] J. van Lierop, K.W. Lin, Z.Y. Guo, B.W. Shouthern, J. Appl. Phys. 99 (2006) 08C101.
[10] C.A.F. Vaz, E.I. Altman, V.E. Henrich, Phys. Rev. B 81 (2010) 104428.
[11] J.B. Tacy, D.N. Weiss, D.P. Dinega, M.G. Bawendi, Phys. Rev. B 72 (2005) 064404.
[12] R.K. Zheng, G.H. Wen, K.K. Fung, X.X. Zhang, J. Appl. Phys. 95 (2004) 5244–5246.
[13] A. Ceylan, C.C. Baker, S.S. Hasanain, S. Ismat Shah, J. Appl. Phys. 100 (2006) 034301.
[14] L.D. Bianco, D. Fiorani, A.M. Testa, E. Bonetti, L. Signorini, Phys. Rev. B 70 (2004) 052401.
[15] Y.Z. Zhou, J.S. Chen, B.K. Tay, J.F. Hu, G.M. Chou, T. Liu, P. Yang, Appl. Phys. Lett. 90 (2007) 043111.
[16] M. Artus, S. Ammar, L. Sicard, J.Y. Piquemal, F. Herbst, M.J. Vanlay, F. Fiévet, V. Richard, Chem. Mater. 20 (2008) 4861–4872.
[17] Z.M. Tian, S.L. Yuan, L. Liu, S.Y. Yin, L.C. Jia, H.N. Duan, P. Li, C.H. Wang, J.Q. Li, Smart Mater. Struct. 18 (2009) 015018.
[18] Y. Zhang, F. Dong, Y. Liu, C.L. Fei, C.X. Pan, D. Yin, R. Xiong, J. Shi, Mater. Chem. Phys. 124 (2010) 1034–1038.
[19] J. Nogués, J. Sort, V. Langlais, S. Doppiu, B. Dieny, J.S. Munoz, S. Surinach, M.D. Baro, S. Stoyanov, Y. Zhang, Int. J. Nanotechnol. 2 (2005) 23–42.
[20] D. Peddis, C. Cannas, G. Piccaluga, E. Agostinelli, D. Fiorani, Nanotechnology 21 (2010) 125705.
[21] L.D. Tung, V. Kolesnichenko, D. Caruntu, N.H. Chou, C.J. O'Connor, L. Spinu, J. Appl. Phys. 93 (2003) 7486–7488.
[22] K. Maaz, M. Usman, S. Karim, A. Mumtaz, S.K. Hasanain, M.F. Bertino, J. Appl. Phys. 105 (2009) 113917.
[23] A. Ceylan, S.K. Hasanain, S. Ismat Shah, J. Phys.: Condens. Matter 20 (2008) 195208.
[24] R.H. Kodama, A.E. Berkowitz, E.J. McNiff Jr., S. Foner, Phys. Rev. Lett. 77 (1996) 394–397.
[25] R.H. Kodama, A.E. Berkowitz, E.J. McNiff Jr., S. Foner, J. Appl. Phys. 81 (1997) 5552–5557.
[26] B. Martinez, X. Obradors, Ll. Balcells, A. Rouanet, C. Monty, Phys. Rev. Lett. 80 (1998) 181–184.

[27] J.H. He, S.L. Yuan, Y.S. Yin, Z.M. Tian, P. Li, Y.Q. Wang, K.L. Liu, C.H. Wang, J. Appl. Phys. 103 (2008) 023906.
[28] S.A. Makhlouf, J. Magn. Magn. Mater. 246 (2002) 184–190.
[29] M.J. Benitez, O. Petracic, E.L. Salabas, F. Radu, H. Tüysüz, F. Schüth, H. Zabel, Phys. Rev. Lett. 101 (2008) 097206.
[30] D.S. Wang, T. Xie, Q. Peng, S.Y. Zhang, J. Chen, Y.D. Li, Chem. Eur. J. 14 (2008) 2507–2513.
[31] R.D. Shannon, Acta Crystallogr. A32 (1976) 1–767.
[32] Y. Zhang, Y. Liu, C.L. Fei, Z. Yang, Z.H. Lu, R. Xiong, D. Yin, J. Shi, J. Appl. Phys. 108 (2010) 084312.
[33] J. Geshev, J. Magn. Magn. Mater. 320 (2008) 600–602.
[34] G. Salazar-Alvarez, J. Sort, S. Suriñach, M. Dolors Baró, J. Nogués, J. Am. Chem. Soc. 129 (2007) 9102–9108.
[35] K. Maaz, A. Mumtaz, S.K. Hasanain, A. Ceylan, J. Magn. Magn. Mater. 308 (2007) 289–295.
[36] M. Vélez, C. Martínez, A. Cebollada, F. Briones, J.L. Vicent, J. Magn. Magn. Mater. 240 (2002) 580–582.
[37] Y.B. Zhang, M.H.N. Assadi, S. Li, J. Phys.: Condens. Matter 23 (2011) 066004.